# Transition from weak wave turbulence to soliton gas

Roumaissa Hassaini and Nicolas Mordant[*]

*Laboratoire des Ecoulements Géophysiques et Industriels, Université Grenoble Alpes,*
*CNRS, Grenoble-INP, F-38000 Grenoble, France*

We report an experimental investigation of the effect of finite depth on the statistical properties of wave turbulence at the surface of water in the gravity-capillary range. We tune the wave dispersion and the level of nonlinearity by modifying the depth of water and the forcing, respectively. We use space-time resolved profilometry to reconstruct the deformed surface of water. When decreasing the water depth, we observe a drastic transition between weak turbulence at the weakest forcing and a solitonic regime at stronger forcing. We characterize the transition between both states by studying their Fourier spectra. We also study the efficiency of energy transfer in the weak turbulence regime. We report a loss of efficiency of angular transfer as the dispersion of the wave is reduced until the system bifurcates into the solitonic regime.

## I. INTRODUCTION

Wave turbulence and solitonic turbulence are two major faces of the propagation of random and weakly nonlinear waves. The dynamics of incoherent dispersive waves has been studied in the framework of the statistical theory of weak turbulence since the pioneering work of Zakharov, Benney, and Newell in the 1960s (see Refs. [1,2] for recent reviews). Based on the hypothesis of weak nonlinearity, the theory predicts an energy transfer through resonant interactions among waves. For forced turbulence it leads most often to a direct energy cascade from the forced large scales to small scales at which dissipation is acting. The weak turbulence theory (WTT) provides analytical predictions of the statistical properties of turbulence such as the stationary wave spectrum. This theory has been applied to many physical systems such as plasmas [3], optics [4], thin elastic plates [5], and geophysical flows [6,7]. In particular, it was applied to waves propagating at the surface of deep water either in the gravity regime [6] or in the capillary regime [8]. In the past decades wave turbulence at the surface of a fluid has been the object of several detailed experimental investigations in either regime or at the gravity-capillary crossover [9–12] that triggered a new dynamics in the field.

For weakly nondispersive waves, weakly nonlinear waves may also develop into solitons, i.e., localized structures that propagate at a constant velocity while keeping their shape unchanged [13]. They were discovered by Russell [14] and modeled by the Korteweg–de Vries (KdV) equation [15]. The interaction between solitons is elastic and appears as a phase shift between pre- and post-collision solitons. When a large number of solitons evolves in a medium, they develop a statistical state called a soliton gas. If soliton gases have been experimentally observed for a long time in optics [16,17], their observation at the surface of fluids has been reported only recently [18,19]. Soliton gases develop a quite different turbulent state than weak turbulence due to the integrability of the KdV equation [20] for which an infinite number of invariants exist in addition to energy.

Here we report the observation of a transition between both weak turbulence and a solitonic regime. We focus on the case of weakly nonlinear waves propagating at the surface of a water layer at scales typical of the gravity-capillary crossover (i.e., wavelengths at centimeter scale). In this configuration weak wave turbulence has been unambiguously reported for a deep enough layer and

---

[*]nicolas.mordant@univ-grenoble-alpes.fr
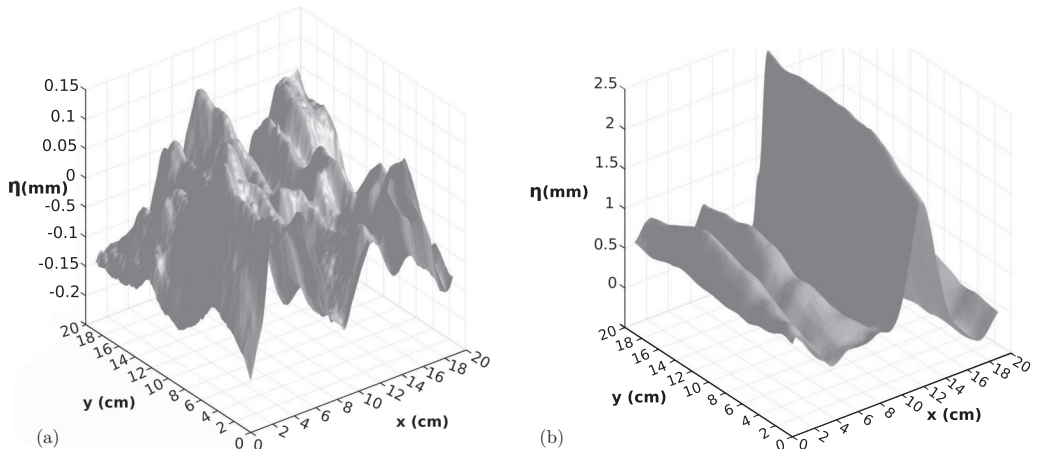
FIG. 1. Elevation field of the waves for a height of water at rest equal to 1 cm. The excitation central frequency is 2 Hz. (a) Amplitude of forcing equal to 0.9 mm. The rms slope is 1.6% and this regime corresponds to wave turbulence. (b) Amplitude of forcing equal to 2.5 mm. The rms slope is 4.1% and a soliton can clearly be identified. In both cases the magnitude of the waves has been magnified strongly vertically.

weak enough forcing using space and time resolved measurements [10,12,21]. Such measurements are required to accurately characterize the wave propagation and identify the nonlinear regimes. At stronger forcing another wave turbulence regime has been identified that is more strongly nonlinear and involves coherent structures [10,22]. Shallow water weak wave turbulence was also observed numerically by di Leoni *et al.* [23] for gravity waves. Furthermore, at finite depth gravity-capillary solitons are known to propagate [24]. We report an investigation of the influence of the water depth and the intensity of the forcing on the statistical properties of wave turbulence. Changing the water depth alters the dispersivity of the waves. We observe and characterize the transition between a weak turbulence regime (low forcing and/or large depth) and a solitonic regime (larger forcing and/or small depth) that may evolve into a soliton gas.

## II. EXPERIMENTAL SETUP

The experimental setup is similar to that of Aubourg and Mordant [12]. It consists of a rectangular $57 \times 37$ cm$^2$ Plexiglas tank filled with water. The depth of water at rest is changed in the range [0.6,6] cm, going from finite depth regimes to deep water regimes considering the centimetric wavelengths. Great care is taken to prevent surface contamination in order to avoid dissipation by conversion to Marangoni waves [25]. The waves are generated by exciting continuously horizontally the container (along its longest axis) using an oscillating table controlled by a sinusoidal tension modulated around a central frequency equal to 2 Hz with a random modulation in an interval $\pm 0.5$ Hz around the central frequency. The deformation of the free surface is reconstructed using Fourier transform profilometry [26,27] (see Ref. [21] for more details of the setup). The water is mixed with titanium dioxide particles at a volume fraction of 1% to improve its optical diffusivity, making it possible to project on its very surface a gray scale sinusoidal pattern. These particles are chemically neutral and do not alter the surface tension of water as stated by Przadka *et al.* [25]. As the waves propagate, the pattern seen by a high speed camera is deformed. The deformation of the pattern can be inverted to provide the elevation field of the waves. In this way we obtain a full space-time resolved measurement of the wave field. The images are recorded at 250 frames/s with a resolution of $1024 \times 1024$ pixels$^2$ covering a 20 cm$^2$ area at the center of the tank.

We perform experiments with various magnitudes of the forcing and several values of the water depth at rest. Figure 1 shows the surface reconstruction in the case of a weak and a strong forcing
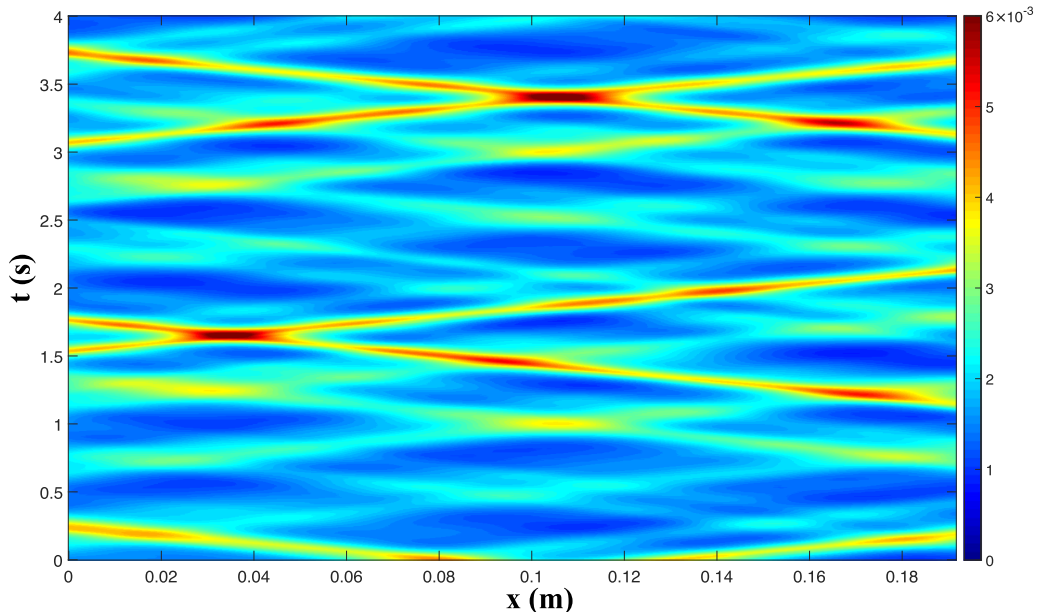
FIG. 2. Space-time plot of the solitonic regime of Fig. 1(b). The excitation central frequency is 2 Hz and the amplitude of forcing is equal to 2.5 mm. The color map is the wave height in meters.

amplitude. At weak forcing, Fig. 1(a) shows a random distribution of the waves. The deformation seems to involve waves coming from all directions. At stronger forcing [Fig. 1(b)] we observe a localized coherent structure. These solitonlike, coherent structures are only propagating along the direction of the oscillation of the table ($x$ axis). Note that there is about a factor of 10 between the amplitudes of the reconstructed waves in both cases. In this regime the system contains actually several solitons which propagate in both directions along the $x$ axis and collide as represented in a space-time representation in Fig. 2.

## III. SPATIOTEMPORAL SPECTRAL ANALYSIS

In order to identify the spectral content of the wave field, we compute the full frequency-wavenumber Fourier spectrum. For a better visualization of the spectra, we actually compute the spectrum of $\frac{\partial \eta}{\partial t}$, which can be interpreted as the vertical velocity due to the weak magnitude of the nonlinearity [$\eta(x,y,t)$ is the instantaneous height of the free surface]. The spectrum is noted $E^v(\mathbf{k},\omega)$ and is shown in Fig. 3 for the two experiments of Fig. 1. At weak forcing [Fig. 3(a)], the energy is concentrated on the dispersion relation of gravity-capillary waves at finite depth:

$$\omega = \sqrt{\left(gk + \frac{\gamma}{\rho}k^3\right)\tanh(kh)},\tag{1}$$

where $\gamma = 72$ mN/m is the surface tension of pure water, $\rho = 10^3$ kg/m$^3$ is the water density, and $g = 9.81$ m/s$^2$ is the acceleration of gravity. At large wavelength $kh \ll 1$, $\omega \approx \sqrt{ghk}$ and the waves are weakly dispersive. The concentration of energy on this linear dispersion relation is the clear indication of the presence of weak turbulence as reported in Refs. [12,21].

At stronger forcing [Fig. 3(b)], when localized structures are present, the energy is concentrated around a straight line of slope $1/c_s$ where $c_s = \sqrt{gh}$. $c_s$ is the velocity expected for solitons. A similar spectral signature has been also reported for solitons in nonlinear optics [28]. In our case the energy is concentrated mostly at large wavelength ($\lambda \gtrsim 2$ cm, corresponding to the size of the
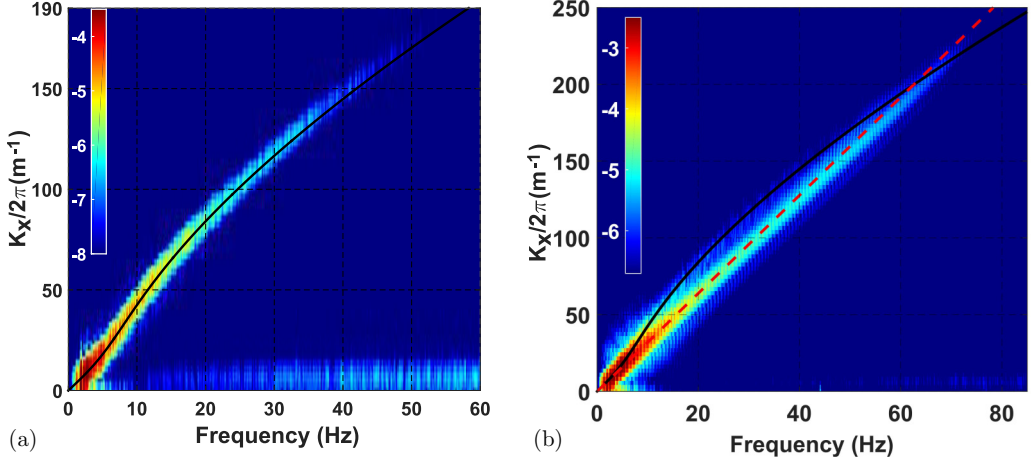
FIG. 3. Space-time Fourier spectrum $E^v(\mathbf{k},\omega) = \langle|v(\mathbf{k},\omega)|^2\rangle$ of the velocity field $v = \frac{\partial\eta}{\partial t}$ of the waves. The height of water at rest is 1 cm. The forcing frequency is centered around 2 Hz. (a) $E^v(k_x, k_y = 0,\omega)$ for an amplitude of forcing equal to 0.9 mm. (b) Same quantity for an amplitude of forcing equal to 2.5 mm. In both (a) and (b), the solid black line is the theoretical finite depth linear dispersion relation for gravity-capillary waves in pure water with surface tension $\gamma = 72$ mN/m. In (b) the dashed red line is a straight line of slope $1/c_s$ with $c_s = \sqrt{gh}$ the celerity of long waves. In both panels the color is the logarithm of $E^v(\mathbf{k},\omega)$.

core of the soliton, $\approx 5$ cm) but it extends down to millimeter wavelengths due to the capillary precursors (reported for gravity-capillary solitons by Falcon *et al.* [24]) that are expected when the Bond number Bo $= \frac{\gamma}{\rho g h^2}$ lies between zero and $1/3$ (which is the case for all our experiments) [29]. At low frequency the spectrum is tangent to the shallow water nondispersive part of the linear dispersion relation but departs clearly from it at smaller wavelengths.

Figure 4 displays cuts of the spectrum $E^v(\mathbf{k},\omega)$ at constant frequency. For deep water ($h = 6$ cm, left column), the spectrum is quite isotropic although the forcing acts along the $x$ axis. This case is very similar to the one previously reported by Aubourg and Mordant [12,21]. It shows a strong angular redistribution of energy. At lower depth and weak forcing [$h = 1$ cm, weak turbulence regime, central column, shown in Figs. 1(a) and 3(a)], the spectra are more anisotropic with energy mostly in the $x$ direction with a much weaker angular spreading. At the same depth but stronger forcing [soliton regime, right column, shown in Figs. 1(b) and 3(b)], energy is only visible on the $x$ axis, along the direction of propagation of the solitons. Furthermore, the peak of energy is clearly out of the linear dispersion as already observed in Fig. 3. A first consequence of reducing the dispersivity of the waves seems to make the angular transfer of energy less efficient until the transition to the soliton regime at which no angular transfer is observed.

We also observe intermediate states between the WTT and the ST represented in Fig. 5, where some energy is observed in between the linear dispersion relation and the solitonic straight dispersion at the celerity $c_s = \sqrt{gh}$. This intermediate stage could be seen only for experiments with finite depths greater than 1 cm and a frequency of forcing lower than 2 Hz. In Fig. 5(a) energy is observed on the linear dispersion relation and below but not yet on the soliton line. Extra energy lines can be seen notably in Fig. 5(b) that correspond to nondispersive structures that propagate at a different velocity. This state corresponds to the beginning of the development of solitons that may not be stable enough to resist the influence of the large scale stationary modes of the tank that possibly tend to make them lose their coherence very quickly. When the amplitude of the forcing is increased the solitonic state is then reached and energy is concentrated around the expected soliton dispersion relation.

As shown in the previous paragraph, the spectral signature of solitons in $(k_x,\omega)$ space corresponds to a straight line that goes through the origin and is tangent to the shallow water gravity-capillary
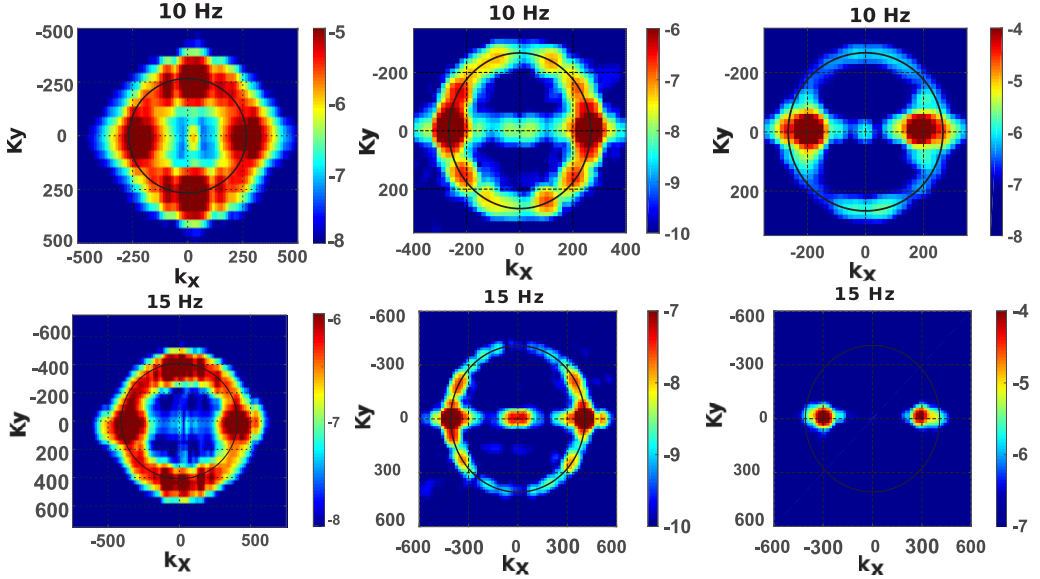
FIG. 4. Cut of the energy spectrum $E^v(k_x,k_y,\omega)$ at a given value of the frequency $F = \omega/2\pi$ and shown as a function of $(k_x,k_y)$. The solid black line corresponds to the finite depth water gravity-capillary dispersion relation (1). The top line corresponds to $F = 10$ Hz and the bottom line corresponds to $F = 15$ Hz. The left column comes from a weakly nonlinear regime in deep water ($h = 6$ cm) where the system is quite isotropic, the central column comes from the WTT experiment in Fig. 3(a), and the right column corresponds to the soliton experiment of Fig. 3(b).

dispersion relation at the lowest frequencies. For a water depth equal to 1 cm [Fig. 3(b)] the line is located below the dispersion relation (for frequencies lower than 60 Hz). For a water depth equal to 6 mm, the energy line representing the soliton is above the dispersion relation as shown in Fig. 6.
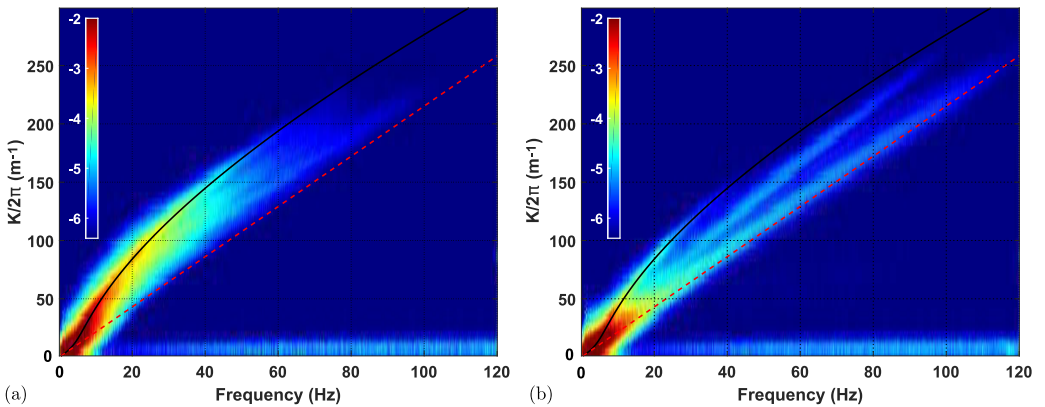


FIG. 5. Space-time Fourier spectrum $E^v(k,\omega)$ of the velocity field of the waves for experiments where the height of water at rest is $h = 3$ cm with a forcing centered around 0.7 Hz in an intermediate regime between weak turbulence and solitonic regime. (a) Amplitude of table oscillation equal to 6.6 mm. The rms slope is 6%. (b) Amplitude of table oscillation equal to 9.2 mm. The rms slope is 6.9%. The solid black line corresponds to the gravity-capillary linear dispersion relation in finite depth for pure water. The red dashed line corresponds to the celerity of the soliton, $c_s = \sqrt{gh}$.
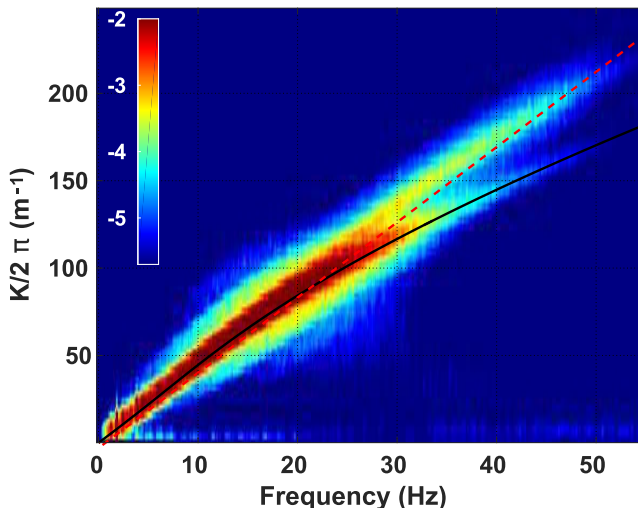
FIG. 6. Space-time Fourier spectrum $E^v(k,\omega)$ of the velocity field of the waves for experiments where the height of water at rest is $h = 6$ mm with a forcing centered around 2 Hz and an amplitude of forcing of 3 mm. The rms slope is measured to be 6.4%. The solid black line corresponds to a finite depth water gravity-capillary linear dispersion relation. The red dashed line corresponds to the celerity of the soliton, $c_s = \sqrt{gh}$.

This represents a transition between a soliton that has a higher celerity than linear waves to a soliton that is slower than linear waves. This is called the bifurcation between the subcritical branch and the supercritical branch as explained by Kuznetsov and Dias in their review [30]. Analytically the inflection point disappears when the Bond number reaches 1/3, i.e., when $h = \sqrt{\dfrac{3\gamma}{\rho g}} = 4.7$ mm for pure water). In Fig. 6 the Bond number is slightly below 1/3 so that the inflection point is barely visible (compared to the spread of energy around the dispersion relation). The dispersion relation is close to linear in a large interval up to about 12 Hz. The soliton energy line is superimposed with the dispersion relation in this interval and then lies above it at higher frequencies. In the previous case of Fig. 3(b) the soliton energy is above the dispersion relation only above 60 Hz. In this configuration we are still in the subcritical case but we clearly see the evolution to the supercritical case.

## IV. FREQUENCY SPECTRA

For pure power law dispersion relations, the weak turbulence theory predicts the expression of the energy spectrum $E(k)$ as

$$E(k) = C P^{1/(N-1)}k^{-\alpha}, \tag{2}$$

where $k = \|\mathbf{k}\|$ is the wave number, $P$ the energy flux, $C$ a dimensional constant that can be calculated, and $\alpha$ the spectral exponent. $N$ is the number of waves taking part in the nonlinear coupling [1]. Using the dispersion relation, one can translate the expression of $k$ spectra into $\omega$ spectra that are often easier to measure. One of the outcomes of WTT is that energy is transmitted among resonant waves. At the lowest order it involves three waves that have then to satisfy the resonance conditions such as $\mathbf{k_1} = \mathbf{k_2} + \mathbf{k_3}$ and $\omega_1 = \omega_2 + \omega_3$. This is the case for pure capillary waves on infinite depth water [8]. In the case of gravity waves the three-wave resonance conditions do not admit solutions because of the negative curvature of the dispersion relation in infinite depth, $\omega = \sqrt{gk}$. One must take into account the next order that involves four waves. The predicted spectra of the surface deformation $\eta$ are thus expected to be

$$E(k) \propto P^{1/3}gk^{-5/2} \tag{3}$$
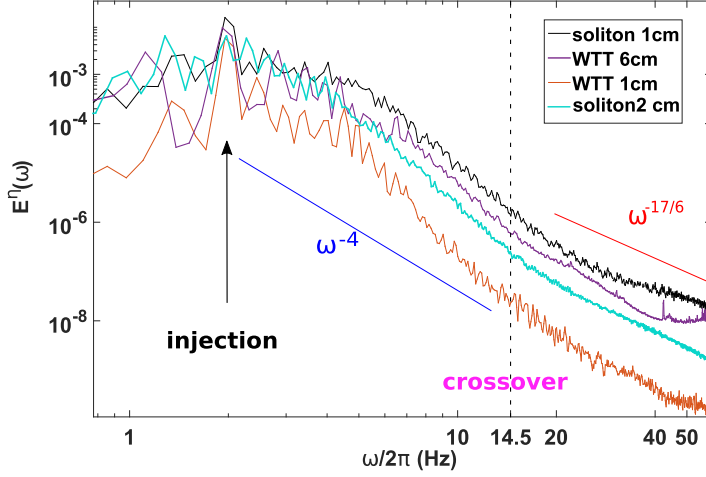
FIG. 7. Time Fourier spectrum $E^v(\omega)$ of the surface deformation for experiments where the height of water at rest is 1 cm with a forcing centered around 2 Hz and an amplitude of forcing equal to 2.5 mm. The vertical dashed line corresponds to the frequency of the crossover between the gravity and the capillary regime for pure water. The injection scale corresponds to the frequency of the forcing.

for deep water pure gravity waves and

$$E(k) \propto P^{1/2} k^{-7/4} \tag{4}$$

for deep water pure capillary waves [1]. Using the dispersion relations for gravity waves and capillary waves in finite depth one can change the variable from $k$ to $\omega$ in the predicted spectra and obtain

$$E(\omega) \propto P^{1/3} g \omega^{-4} \tag{5}$$

for gravity waves and

$$E(\omega) \propto P^{1/2} \left( \frac{\gamma}{\rho} \right)^{1/6} \omega^{-17/6} \tag{6}$$

for capillary waves. Laboratory experiments fail to reproduce this prediction for the gravity waves. In large or small wave tanks, the spectral exponent of the gravity waves is seen to vary strongly with the forcing intensity and to be close to the WTT predictions only at the highest forcing magnitude, in opposition to the weak nonlinearity hypothesis [9,31]. For capillary waves, experiments seem to follow better the predictions of the WTT [32,33].

Figure 7 shows the frequency spectra for various experimental configurations. The spectra corresponding to a weak turbulence regime (at 1 and 6 cm depth) are very similar to that of Aubourg and Mordant [21]. At frequencies below the gravity-capillary crossover (at 14.5 Hz) and thus corresponding to gravity waves the spectra are steeper than the WTT prediction, the steepest being observed at low depth. In the capillary range, the spectra are also steeper than the WTT prediction, consistent with Aubourg and Mordant [21] but at odds with observation by Falcon *et al.* [11], who observed a $\omega^{-3}$ scaling close to the WTT prediction. In the solitonic regime, the spectrum is not changed much in the gravity range. In the capillary range the spectra are changed and are closer to the WTT prediction and even less steep at 1 cm depth. This may suggest that the $\omega^{-3}$ scaling observed by Falcon *et al.* may correspond to the strong regime reported by Cobelli *et al.* [10]. In their Fig. 1 (top, strong regime) the surface velocity shows coherent structures that may be some sort of gravity-capillary solitons generated by the paddles even if their water depth is not that small (5 cm). The $\omega^{-3}$ scaling may be due to the solitons as it is the case in our experiment at 2 cm water depth rather than being due to a fulfillment of the WTT prediction.
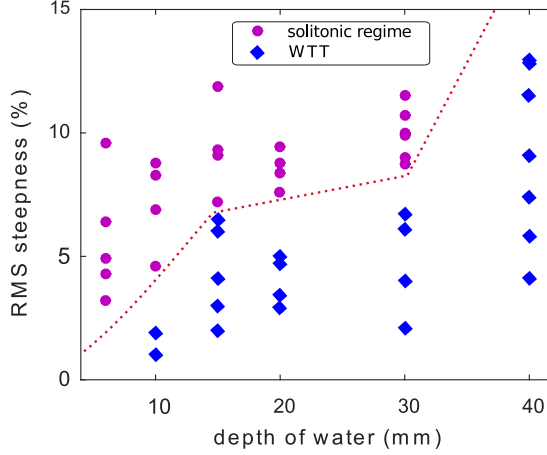
FIG. 8. Solitonic transition phase diagram represented as a function of the rms steepness of the waves and the depth of water at rest, for experiments where the central frequency of excitation is 2 Hz. The dashed red line distinguishes the area where localized structures are predominant from the one where random waves are predominant.

## V. PHASE DIAGRAM

The solitons that have been observed in our work are expected to follow the Korteweg–de Vries equation:

$$\eta_t + \frac{3}{2}\frac{c_s}{h}\eta\eta_\xi + \frac{1}{6}c_s h^2\left(\frac{1}{3} - \text{Bo}\right)\eta_{\xi\xi\xi} = 0, \tag{7}$$

with $c = c_s(1 + \frac{\eta_0}{2h})$ and $\xi = x - ct$. Note that $\eta_0 < 0$ when $\text{Bo} > \frac{1}{3}$, $\eta_0 > 0$ when $0 \leqslant \text{Bo} < \frac{1}{3}$. Equation (7) can be derived only if nonlinear effects are small and have the same order of magnitude as dispersive ones. Dispersion is quantified by $\mu = (\frac{h}{L})^2$ and the nonlinearity is quantified using the typical rms steepness of the waves:

$$\epsilon \equiv \sigma = \left\langle \sqrt{\frac{1}{S}\int_S \|\nabla\eta(x,y,t)\|^2 \; dx\,dy} \right\rangle. \tag{8}$$

Figures 1 and 3 pointed out major changes in the spatial and spectral signatures of the studied states where only the amplitude of the forcing was tuned. Figure 8 displays a phase diagram of the weak turbulence regime and the solitonic one as a function of the water depth and the measured steepness of the waves. The central frequency is kept constant and equal to 2 Hz for all the experiments. At a given water depth, the central frequency imposes indirectly the size of the soliton although predicting the actual size involves computing the inverse scattering transform of the excitation [34]. This computation is beyond the scope of this article but we observe that the size of the soliton changes only weakly with the experimental parameters. Thus the water depth is a measure of the dispersivity of the waves while the steepness is a measure of the nonlinearity. Each case is categorized as either solitonic or weakly turbulent by the observation of the Fourier spectrum. A border is clearly observed between both regimes. The border is increasing with the water depth: for deeper water it requires to force stronger waves to observe solitons. Equality between nonlinearity and dispersion is expected at the border, since it is the required condition for the development of solitary waves. To verify this condition we display in Table I the minimal values of nonlinearity and dispersion for which solitary waves were observed for different values of the water depth. Globally we observe that the balance between nonlinearity and dispersion is fulfilled at each depth of water. Dispersion

TABLE I. Values of the nonlinearity $\epsilon$ and the dispersion $\mu$ for different depths of water with a frequency of excitation $\in [1.5\ 2.5]$ Hz. $\epsilon$ is estimated by directly measuring the surface averaged rms steepness of the waves. $\mu = (\frac{h}{L})^2$ is computed by measuring the depth of water at rest, $h$, and $L$, the typical size of the core of the soliton.

| $h$ (cm) | 0.6 | 1 | 1.5 | 2 | 3 | 4 |
|---|---|---|---|---|---|---|
| $\epsilon$ (%) | 3.2 | 4.6 | 7.3 | 7.6 | 8.8 | ∄ |
| $\mu$ (%) | 3.8 | 4 | 7.2 | 7.3 | 9 | ∄ |

is defined as $\mu = (\frac{h}{L})^2$ where $L$ is the length of the core of the soliton. As $L$ is weakly changing it means that when the depth of water is increased the dispersion is stronger. The condition of balance of dispersion and nonlinearity imposes that the nonlinearity should be stronger as well in order to observe the solitons. In the deepest case ($h = 4$ cm) it was not possible to observe solitons as the nonlinearity was becoming very high and the waves were close to overturning.

## VI. ANGULAR ENERGY TRANSMISSION

Although the transition between the two regimes seems very abrupt, the observation of the wave spectrum showed a progressive change in the angular transfer of energy in the weak turbulence regime when decreasing the water depth. For truly nondispersive waves (acoustic waves), the resonant manifold involves only waves propagating in the same direction. Thus Newell and Rumpf asked the question of the evolution of an initially anisotropic distribution of waves [2]. Would higher order terms lead to angular transfer of energy or would the energy be condensed on rays that would evolve into shocks? Here we decrease progressively the dispersion of the waves and we clearly
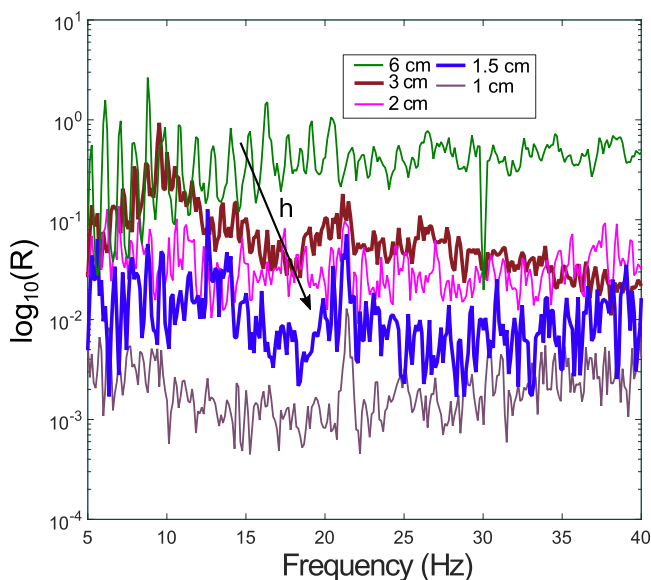


FIG. 9. Evolution of the ratio $R(\omega) = \frac{E^v(k_x=0,k_y(\omega))}{E^v(k_x(\omega),k_y=0)}$ of the energy perpendicular to the direction of the forcing oscillation over the energy in the direction of the forcing and for different depths $h$ of water. The energy level is taken on the linear dispersion relation $k(\omega)$. The central frequency of excitation is equal to 2 Hz. The rms steepnesses of the surface for values of the water depth $h = [6, 3, 2, 1.5, 1]$ cm are respectively $[4.4, 6.5, 5, 6.4, 4.1]\%$. In all cases the wave steepnesses are thus close to 5%.

see that the efficiency or angular transfer is altered. In order to be more quantitative we define $R$ as the ratio of the energy of the waves transverse to the forcing ($k_x = 0$) divided by the energy of longitudinal waves propagating in the direction of the forcing ($k_y = 0$):

$$R(\omega) = \frac{E^{\upsilon}(k_x = 0, k_y(\omega))}{E^{\upsilon}(k_x(\omega), k_y = 0)}, \tag{9}$$

where $k(\omega)$ is the linear dispersion relation. Aubourg and Mordant [12] reported for deep water that, although the energy injection is strongly anisotropic by forcing mostly waves in the $x$ direction, the nonlinear interactions between the waves redistribute isotropically this energy in a very efficient way. We show the evolution of $R(\omega)$ in Fig. 9. We chose data sets for which the wave steepness (measure of the nonlinearity) is almost the same and close to 5% in order to show only the effect of changing the dispersion of the waves. Consistently with the observation of Aubourg and Mordant, $R$ is close to 1 in the deepest case. $R$ decays strongly when the water depth evolves from 6 down to 1 cm. This decay is roughly the same at all frequencies. When the water depth is 1.5 cm, the ratio $R$ decayed by a factor of 100. At 1 cm water depth the system transited into the soliton regime. In that regime the ratio is down to $10^{-3}$, showing that almost no directional transfer of energy is occurring. Answering Newell and Rumpf, for finite depth gravity-capillary waves no angular transfer is induced by higher order closure but the system develops solitons rather than shocks as a weak dispersion remains present in our case.

## VII. CONCLUSIONS

In summary, we investigated the impact of nonlinearity and wave dispersion on wave turbulence. For strong dispersion of the waves (large water depth) and weak nonlinearity we observe a state of weak turbulence. When the dispersion of the waves is weak, the strength of nonlinearity can match that of dispersion. In these conditions, we observe the generation of solitons and thus a change of statistical regime from weak turbulence to soliton gas. The fate of energy is thus expected to be quite different. For weak turbulence, through resonant interactions, energy cascades to very small scales at which it is dissipated. In the absence of dissipation, solitons propagate without changing their shape and their interaction is elastic. An ensemble of solitons evolves into a state of integrable turbulence [20,35] which has properties distinct from that of weak turbulence. Although in fiber optics the soliton gas is restricted to one-dimensional propagation, for gravity-capillary waves solitons can have a two-dimensional propagation and this may be the case of the state observed by Cobelli *et al.* [10] at their strongest forcing. Note that Zakharov *et al.* predicted [36] that, for unidirectional propagation of gravity waves in deep water, weak turbulence should be unstable and coexist with solitonlike structures. In our case no coexistence of solitons and weak turbulence has been observed except very near the transition. We observe two very distinct regimes.

## ACKNOWLEDGMENTS

---

[1] S. Nazarenko, *Wave Turbulence*, Vol. 825 (Springer, New York, 2011).

[2] A. C. Newell and B. Rumpf, Wave turbulence, Annu. Rev. Fluid Mech. **43**, 59 (2011).

[3] R. Z. Sagdeev, The 1976 Oppenheimer lectures: Critical problems in plasma astrophysics. I. Turbulence and nonlinear waves, Rev. Mod. Phys. **51**, 1 (1979).

[4] A. Picozzi, J. Garnier, T. Hansson, P. Suret, S. Randoux, G. Millot, and D. N. Christodoulides, Optical wave turbulence: Towards a unified nonequilibrium thermodynamic formulation of statistical nonlinear optics, Phys. Rep. **542**, 1 (2014).

[5] G. Düring, C. Josserand, and S. Rica, Weak Turbulence for a Vibrating Plate: Can One Hear a Kolmogorov Spectrum? Phys. Rev. Lett. **97**, 025503 (2006).

[6] K. Hasselmann, On the non-linear energy transfer in gravity-wave spectrum. Part 1. General theory, J. Fluid Mech. **12**, 481 (1962).

[7] S. Galtier, Weak inertial-wave turbulence theory, Phys. Rev. E **68**, 015301 (2003).

[8] V. E. Zakharov and N. N. Filonenko, Weak turbulence of capillary waves, J. Appl. Mech. Tech. Phys. **8**, 37 (1967).

[9] S. Nazarenko, S. Lukaschuk, S. McLelland, and P. Denissenko, Statistics of surface gravity wave turbulence in the space and time domains, J. Fluid Mech. **642**, 395 (2009).

[10] P. Cobelli, A. Przadka, P. Petitjeans, G. Lagubeau, V. Pagneux, and A. Maurel, Different Regimes for Water Wave Turbulence, Phys. Rev. Lett. **107**, 214503 (2011).

[11] E. Falcon, Laboratory experiments on wave turbulence, Discrete Contin. Dyn. Syst. Ser. B **13**, 819 (2010).

[12] Q. Aubourg and N. Mordant, Nonlocal Resonances in Weak Turbulence of Gravity-Capillary Waves, Phys. Rev. Lett. **114**, 144501 (2015).

[13] M. Peyrard and T. Dauxois, *Physique des Solitons* (EDP Sciences, Les Ulis, France, 2004).

[14] J. S. Russell, *Report on Waves: Made to the Meetings of the British Association in 1842-43* (Richard and John E Taylor, London, 1845).

[15] D. J. Korteweg and G. De Vries, XLI. On the change of form of long waves advancing in a rectangular canal, and on a new type of long stationary waves, London Edinburgh Dublin Philos. Mag. J. Sci. **39**, 422 (1895).

[16] A. Schwache and F. Mitschke, Properties of an optical soliton gas, Phys. Rev. E **55**, 7720 (1997).

[17] F. Mitschke, I. Halama, and A. Schwache, Soliton gas, Chaos Solitons Fractals **10**, 913 (1999).

[18] A. Costa, A. R. Osborne, D. T. Resio, S. Alessio, E. Chrivi, E. Saggese, K. Bellomo, and C. E. Long, Soliton Turbulence in Shallow Water Ocean Surface Waves, Phys. Rev. Lett. **113**, 108501 (2014).

[19] S. Perrard, L. Deike, C. Duchêne, and C.-T. Pham, Capillary solitons on a levitated medium, Phys. Rev. E **92**, 011002 (2015).

[20] V. E. Zakharov, Turbulence in integrable systems, Stud. Appl. Math. **122**, 219 (2009).

[21] Q. Aubourg and N. Mordant, Investigation of resonances in gravity-capillary wave turbulence, Phys. Rev. Fluids **1**, 023701 (2016).

[22] M. Berhanu and E. Falcon, Space-time-resolved capillary wave turbulence, Phys. Rev. E **87**, 033003 (2013).

[23] P. Clark di Leoni, P. J. Cobelli, and P. D. Mininni, Wave turbulence in shallow water models, Phys. Rev. E **89**, 063025 (2014).

[24] É. Falcon, C. Laroche, and S. Fauve, Observation of Sommerfeld Precursors on a Fluid Surface, Phys. Rev. Lett. **91**, 064502 (2003).

[25] A. Przadka, B. Cabane, V. Pagneux, A. Maurel, and P. Petitjeans, Fourier transform profilometry for water waves: How to achieve clean water attenuation with diffusive reflection at the water surface? Exp. Fluids **52**, 519 (2011).

[26] P. J. Cobelli, A. Maurel, V. Pagneux, and P. Petitjeans, Global measurement of water waves by Fourier transform profilometry, Exp. Fluids **46**, 1037 (2009).

[27] A. Maurel, P. Cobelli, V. Pagneux, and P. Petitjeans, Experimental and theoretical inspection of the phase-to-height relation in Fourier transform profilometry, Appl. Opt. **48**, 380 (2009).

[28] J. Laurie, U. Bortolozzo, S. Nazarenko, and S. Residori, One-dimensional optical wave turbulence: experiment and theory, Phys. Rep. **514**, 121 (2012).

[29] R. Grimshaw, Solitary waves with oscillatory tails and exponential asymptotics, in *Geometrical Methods in Fluid Dynamics*, Vol. 34 (Woods Hole Oceanographic Institute, Woods Hole, MA, 1993), pp. 292–298.

[30] E. A. Kuznetsov and F. Dias, Bifurcations of solitons and their stability, Phys. Rep. **507**, 43 (2011).

[31] E. Falcon, C. Laroche, and S. Fauve, Observation of Gravity-Capillary Wave Turbulence, Phys. Rev. Lett. **98**, 094503 (2007).

[32] W. B. Wright, R. Budakian, D. J. Pine, and S. J. Putterman, Imaging of intermittency in ripple-wave turbulence, Science **278**, 1609 (1997).

[33] L. Deike, M. Berhanu, and E. Falcon, Decay of capillary wave turbulence, Phys. Rev. E **85**, 066311 (2012).

[34] S. Trillo, G. Deng, G. Biondini, M. Klein, G. F. Clauss, A. Chabchoub, and M. Onorato, Experimental Observation and Theoretical Description of Multisoliton Fission in Shallow Water, Phys. Rev. Lett. **117**, 144102 (2016).

[35] S. Randoux, P. Walczak, M. Onorato, and P. Suret, Intermittency in Integrable Turbulence, Phys. Rev. Lett. **113**, 113902 (2014).

[36] V. Zakharov, F. Dias, and A. Pushkarev, One-dimensional wave turbulence, Phys. Rep. **398**, 1 (2004).